Effect of the electrode to work angle, filler diameter and shielding gas type on weld geometry of HQ130 steel joints produced by robotic GMAW

H.R. Ghazvinloo[1], A. Honarbakhsh-Raouf[1] and N.Shadfar[2]

[1]*Dept. of Materials Engineering, Semnan University, Semnan, Iran*
[2]*Oghab Afshan Indust. and Man. Co., Semnan, Iran*
hamid.ghazvinloo@gmail.com; ahonarbakhsh@semnan.ac.ir; nasim.shadfar@oghabafshan.com

Abstract

GMAW (Gas Metal Arc Welding) is an arc welding process which is widely used in industry to join the metals. We investigated the effect of varying welding parameters on the bead geometry in robotic GMA welds of HQ130 steel having 5 mm thickness. The chosen parameters for this study were the electrode to work angle (Φ), filler diameter (d) and shielding gas type (S.G). Different samples obtained by employing electrode to work angle of 65°, 75° and 85°, filler diameter of 0.8, 1, 1.2 mm. The main recommended gases for this filler material type were Ar, He and CO_2 gas. Having finished the welding process, the depths of penetration were measured for specimens and the relationship between parameters and penetration of weld were studied. The results clearly illustrated that increasing of electrode to work angle increases the depth of penetration while increasing in filler diameter results in decreasing the weld penetration. In addition, the highest penetration was observed for CO_2 shielding gas.

1. Introduction

GMAW process is an important component in many industrial operations (HG *et al*., 2003). This process is versatile, since it can be applied for all welding positions; it can easily be integrated into the robotized production canters. These advantages have motivated many researchers to study GMAW process in detail (Messler, 1999). This process involves large number of interdependent variables that can affect product quality, productivity and cost effectiveness. The relationship between process variables and bead geometry are complex because of the number of variables and their interrelationships involved. Many attempts have been made to predict and understand the effect of the welding variables on the bead geometry. These include the entire theoretical studies based on heat flow theory (Rosenthal, 1941; Roberts & Wells, 1954; Christensen *et al*., 1965; Friedman & Glickstein, 1976; Zacharia *et al*., 1988; Tsao & Wu, 1988) and the empirical methods based on studies of actual welding applications (Drayton, 1972; Jones, 1976; Doherty & McGlone, 1977; Shinoda & Doherty, 1978; McGlone, 1978; McGlone & Chadwick, 1978; Doherty, 1978; Chandel, 1988; Yang *et al*., 1993).

Steel HQ130 is one of the high strength steels and its tensile strength is more than 1300 MPa (Ashby & Easterling, 1982) and is newly developed low carbon quenched-and-tempered steel used for engineering machinery (Juan *et al*., 2003). Investigation into the relationship between the welding process parameters and bead geometry began in the Mid 1900s and regression analysis was applied to welding geometry research by Lee & Um (2000); Raveendra & Parmar (1987). Kim *et al*. (2003) developed the mathematical models explaining relationship between process variables and bead penetration of bead-on-plate welds and select the best model for controlling the robotic CO_2 arc welding process. The effects of welding current, arc voltage and welding speed on the penetration of Erdemir 6842 steel welded by GMA welding process were researched by Karadeniz *et al*. (2007). Gao *et al*. (2007) shown that full weld penetration denoting efficient synergetic effect only can be obtained under the appropriate shielding gas parameters. Mostafa & Khajavi (2006) optimized the FCAW welding parameters to maximize weld penetration. However, nearly there exists few informations about welding research in super-high strength steel especially relationship between welding parameters and penetration in the available literatures. The present paper has attempted to study the effect of process parameters on bead penetration of joints produced by robotic GMA welding.

2. Materials and methods

Due to high application in industry, welding specimens were prepared from HQ130 steel plates having 5 mm thickness. The chemical composition of base metal has been shown in Table 1. The ER70S-6 (AWS A5.18 Classification) consumable wire selected as filler metal since it has been most widely used in different industrial applications. The selection of the welding electrode wire was based principally upon matching the mechanical properties and physical characteristics of the base metal, weld size and existing electrode inventory (Kim *et al.*, 2003). Chemical composition of the filler metal has been indicated in Table 2. In order to minimize weld distortion, before welding operation, experimental test plates were located in the fixture jig.

Table 1. *The chemical composition of steel HQ130*

Elements	C	Si	Mn	Mo	
Wt (%)	0.176	0.275	1.221	0.284	
	Cr	Ni	B	S	P
	0.55	0.03	0.0013	0.0058	0.027

Specimens used in this investigation were extracted from single butt-welded joints. GMA welding operations were performed by means of a SOS Model DR Series ARK ROBO 1500 welding robot having a working capacity of 0-600A and 0-50V ranges. The welding robot and its apparatus have been shown in Fig. 1.

Table 2. *The chemical composition of filler metal*

Elements	P	S	Si	Mn	C	Cu
Wt (%)	0.035	0.025	0.95	1.63	0.11	0.5

Fig.1. *The GMA welding robot and its apparatus used in experiments*

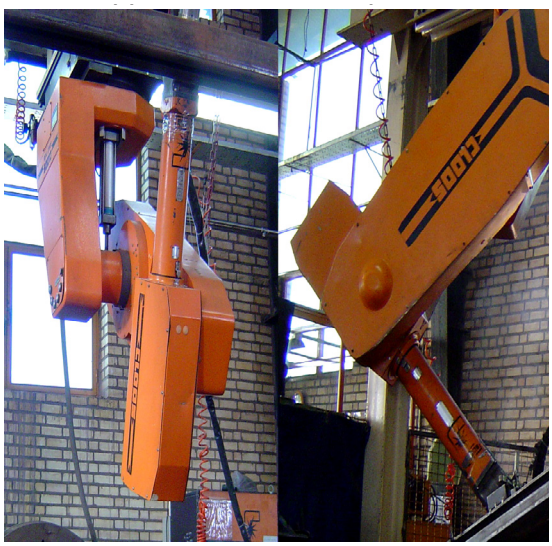

The chosen variables for this study were the electrode to work angle, filler diameter and shielding gas type and the response was bead penetration. These parameters and limits employed were given in Table 3.

Table 3. *Process parameters and limits*

Parameter	Limits/Type
electrode to work angle (Φ)	65°, 75°, 85°
filler diameter (d)	0.8, 1, 1.2 mm
shielding gas (S.G)	Ar, He, CO_2

The welding parameters which have been used unchanged in all welding conditions have been given in Table 4.

Table 4. *Welding parameters were used during to the welding*

Parameter	Limit/Type
Cylinder pressure (bar)	135
Cylinder outlet pressure (L/min)	14
Nozzle opening (mm)	10
Electrode stick out (mm)	15
Arc length (mm)	3
Nozzle-to-work distance (mm)	16
Arc voltage (V)	23
Welding current (A)	140
Welding speed (cm/min)	60
Wire feeding rate (m/min)	8
Droplet transfer	Spray Transfer mode
Polarity	DCEP

After the welding process, the specimens were cut perpendicular to welding direction by using a power hacksaw then the end faces were machined. End faces were removed from any combination and then polished and etched using a 2.5% nital solution in order to measure the depth of penetration. A schematic illustration of bead penetration in welding applications has been shown in Fig. 2.

Fig.2. *A schematic illustration of weld penetration (Kim et al., 2003)*

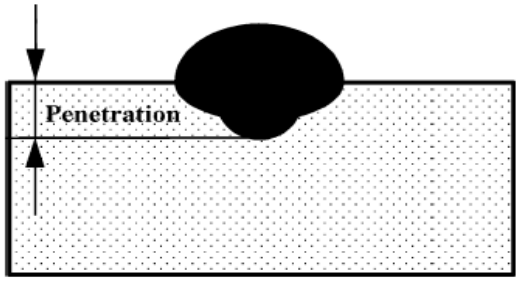

3. Results and discussion

Totally 9 experiments with different electrode to work angle, filler diameter and shielding gas combinations were performed and the depth of penetration was measured for all cases. The results were tabulated as in Figs. 3-5. To determine the effect of each parameter on weld penetration, all other parameters were fixed in accordance with Table 5.

Fig.3. *Penetration vs. the electrode to work angle diagram for 1.6mm filler diameter and CO2 gas*

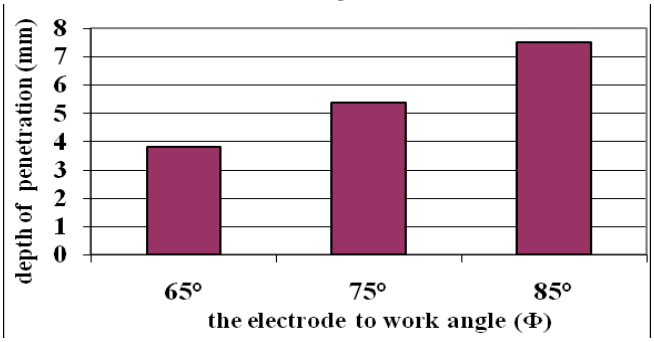

Fig.4. *Penetration vs. filler diameter diagram for 80° electrode to work angle and CO2 shielding gas*

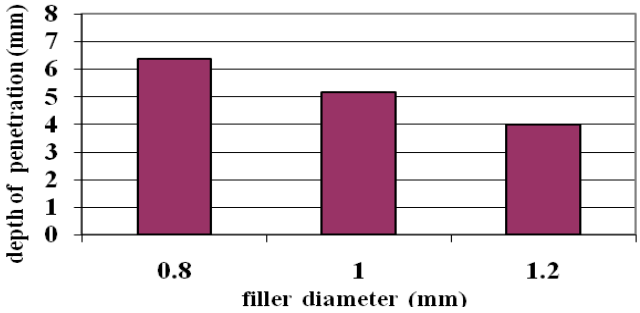

Fig.5. *Penetration vs. shielding gas type diagram for 80° the electrode to work angle and 1.6mm filler metal diameter*

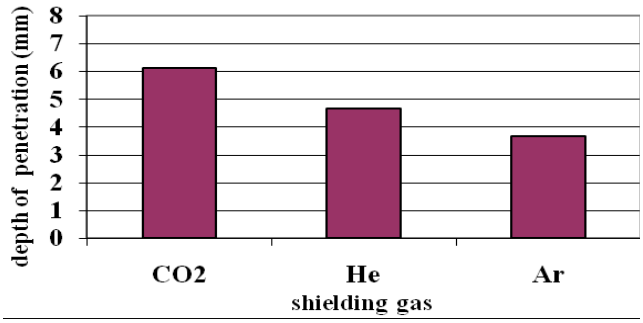

3.1 The effect of electrode to work angle on penetration

The effect of electrode to work angle on depth of penetration was commented according to the results shown in Fig. 3. In Fig. 3, the filler diameter was fixed as 1.6 mm and CO_2 gas was selected as shielding gas and the change in depth of penetration was drawn with increasing the electrode to work angle for 65°, 75° and 85°. According to Fig. 3, it was clearly seen that the depth of penetration values increased with increasing in electrode to work angle from 65° to 85° and these values were 3.81, 5.38 and 7.50 mm.

Table 5. *The fixed parameters in every section of research*

Aim	Fixed parameters
To determine the effect of electrode to work angle on weld penetration	d=1.6mm, S.G = CO_2
To determine the effect of filler diameter on weld penetration	Φ=80°, S.G = CO_2
To determine the effect of shielding gas type on weld penetration	Φ=80°, d = 1.6 mm

In a high electrode to work angle, only the butt joint root is directly affected by arc heat, however, decreasing the angle, results in deviation of arc focusing from joint root and tends to be wasted on previous weld line in drag welding state. On the other hand, arc spacing shape is normally conical in which decreasing the angle increases the base of cone and increasing the contact surface between arc and workpiece. Therefore, in constant arc length and welding heat input, the applied heat per area decreased and this results in a reduction of the penetration ability of weld metal.

3.2 The effect of filler diameter on penetration

The effect of filler diameter on depth of penetration was commented according to the results shown in Fig. 4. Here, the electrode to work angle was fixed as 80° and CO_2 gas was selected as shielding gas and the change in penetration was drawn with increasing filler diameter for 0.8, 1 and 1.2mm. According to Fig. 4, the depth of penetration values decreased with increasing in filler diameter from 0.8 to 1.2 and these values were 6.36, 5.18 and 4mm.

The effect of filler diameter on weld penetration can be related to drop size separated from filler top. With increasing the filler diameter, weld drop size increases in constant arc length and heat input and big drops have poor penetration ability in compare to small drops. Also, the intensity of arc focusing on joint root decreases with increasing the filler metal diameter.

3.3 The effect of shielding gas type on penetration

The effect of type of shielding gas on depth of penetration was shown in Fig. 5. According to Fig. 5, it was clearly shown when CO_2 gas was chosen as shielding gas, the highest penetration was obtained while the penetration obtained for Ar gas was minimum value in this research. The penetration values were 6.13, 4.68 and 3.69mm for CO_2, He and Ar gas, respectively.

Argon and helium are inert gases. The density of argon is approximately 1.4 times that of air (heavier) while the density of helium is approximately 0.14 times that of air (lighter). The heavier the gas the more effective it is at any given flow rate for shielding the arc and blanketing the weld area in flat position (downhand) welding. Helium possesses a higher thermal conductivity than argon and also produces an arc plasma in which the arc energy is more uniformly dispersed. The argon arc plasma is characterized by a very high energy inner core and an outer mantle of lower heat energy. This difference strongly affects the weld bead profile. The helium arc produces a deep, broad, parabolic weld bead. Carbon dioxide (CO_2) is a reactive gas. With a CO_2 shield, metal transfer is either of the short circuiting or globular mode. Axial spray transfer is a characteristic of the argon shield and cannot be achieved with a CO_2 shield. The globular type transfer arc is quite harsh and produces a rather high level of spatter. This requires that the welding conditions be set with relatively low voltage to provide a very short "buried arc" (the tip of the electrode is actually below the surface of the work), in order to minimize spatter. In overall comparison to the argon, helium and CO_2 gases, the CO_2-shielded arc produces a weld bead of excellent penetration with a rougher surface profile and much less "washing" action at the extremity of the weld bead due to the buried arc. Very sound weld deposits are achieved but mechani-

cal properties may be adversely affected due to the oxidizing nature of the arc (American Welding Society, 1997).

4. Microstructure

The metallographic test was used to measure of penetration depth in GMA welded samples. Depth of penetration was measured by optical microscope 10× magnification. The resulted light of macro-structure photos were given in Figs. 6–14. The metallographic test clearly illustrated that there is LOP (lack of penetration) defect in joint root in some configurations like in Figs. 6, 9 and 12. Depth of penetration in these samples was lower than that of others so that welding conditions similar to Figs. 6, 9 and 12 are not suitable and result to a poor weld bead in joint root. Figs. 7, 10 and 13 seem to be the optimum configurations. Depth of penetration in these samples was good and penetration was complete. Over-penetrated samples were shown in Figs. 8, 11 and 14. Over-penetration is an unnecessary situation and result in waste of material and production costs rise. Also increase the weight of construction and structure becomes heavier. These are undesired events, so it is essential to prevent from over-penetration (Karadeniz *et al*., 2007).

Fig. 6. Φ = 65°, d = 1.6 mm, S.G = CO2 condition. Depth of penetration P =3.81mm ×10.

Fig. 9. Φ = 80°, d = 1.2 mm, S.G = CO2 condition. Depth of penetration P =4mm ×10.

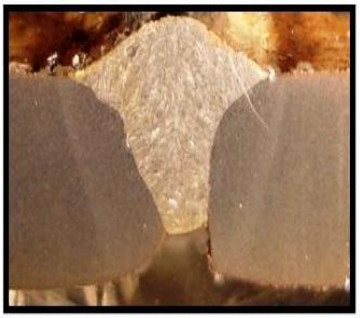

Fig. 12. Φ = 80°, d = 1.6 mm, S.G = Ar condition. Depth of penetration P =3.69mm ×10.

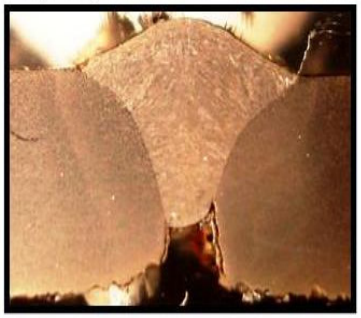

Fig. 7. Φ = 75°, d = 1.6 mm, S.G = CO2 condition. Depth of penetration P =5.38mm ×10.

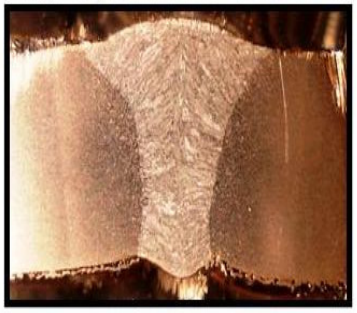

Fig. 10. Φ = 80°, d = 1 mm, S.G = CO2 condition. Depth of penetration P =5.18mm ×10.

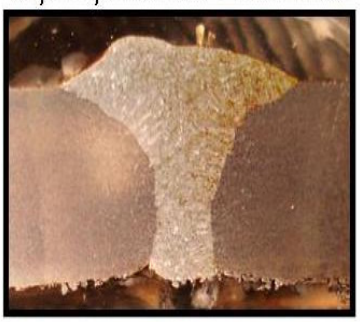

Fig. 13. Φ = 80°, d = 1.6 mm, S.G = He condition. Depth of penetration P =4.68mm ×10.

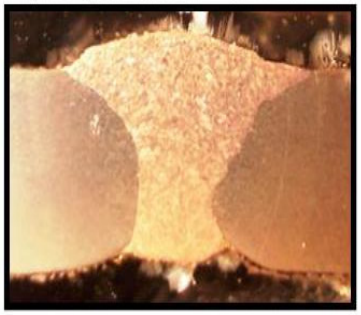

Fig. 8. Φ = 85°, d = 1.6 mm, S.G = CO2 condition. Depth of penetration P =7.5mm ×10.

Fig. 11. Φ = 80°, d = 0.8 mm, S.G = CO2 condition. Depth of penetration P =6.36mm ×10.

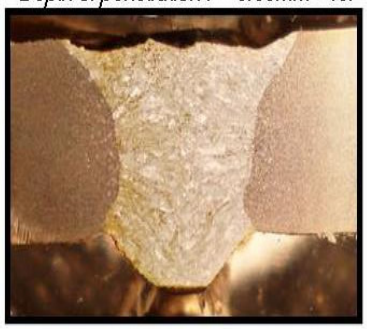

Fig. 14. Φ = 80°, d = 1.6 mm, S.G = CO2 condition. Depth of penetration P =6.13mm ×10.

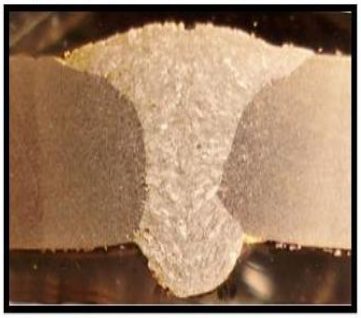

5. Conclusions

According to the results obtained from robotic GMA welding applied to HQ130 steel sheet having 5mm thickness:

(1). The depth of penetration increased from 3.81 to 7.5 mm with increasing the electrode to work angle from 65° to 85°. The optimum condition was for 75° the electrode to work angle.

(2). The depth of penetration decreased from 6.36 to 4mm with increasing the filler diameter from 0.8 to 1.2 mm and the optimum state was for 1 mm filler diameter.

(3). Among CO_2, He and Ar gas as used shielding gases in this research, the deepest and lowest penetration values were 6.13 and 3.69 mm which were seen for CO_2 and Ar gas, respectively.

6. Acknowledgement

The authors thank Industrial & Manufacturing Company of OGHAB AFSHAN for their financial support and Semnan University for all the facilities.

7. References

1. American Welding Society (1997) MIG/MAG Welding Guide. Lincoln Electric CO., Third Edition.
2. Ashby MF and Easterling KE (1982) A first report of microstructure and hardness for heat-affected zones. *J. Acta Metall*. 30, 1969–1978.
3. Chandel RS (1988) Mathematical modeling of gas metal arc weld features, Palm Coast, FL. *Proc. 4thIntl. Conf. on Modeling of Casting & Welding Processes*. 109–120.
4. Christensen N, de V, Davies L and Gjermundsen K (1965) Distribution of temperatures in arc welding. *Brit. Weld J*. 12, 54–75.
5. Doherty J and McGlone JC (1977) Relationships between process variables and weld geometry. *Welding Institute Report*. 52/1977/PE.
6. Doherty J, Shinoda T and Weston J (1978), The relationships between arc welding parameters and fillet weld geometry for MIG welding with flux cored wires. *Welding Institute Report*. 82/1978/PE.
7. Drayton PA (1972) An examination of the influence of process parameters on submerged arc welding. *Welding Instt. Res. Report*. PE4/72.
8. Friedman E and Glickstein SS (1976) An investigation of the thermal response of stationary gas tungsten arc weld. *Weld J*. 55, 12, 408-s–420-s.
9. Gao M, Zeng X and Hu Q (2007) Effects of gas shielding parameters on weld penetration laser-TIG hybrid welding of CO_2. *J. Mater.Process.Technol*. 184, 177–183.
10. HG M and *et al*. (2003) Acquisition and pattern recognition of spectrum information of welding metal transfer. *J. Mater.& Des*. 24, 699–703.
11. Jones SB (1976) Process tolerance in submerged arc welding. *Welding Institute Res. Report*. 1/1976/PE.
12. Juan W, Yajiang L and Peng L (2003) Effect of weld heat input on toughness and structure of HAZ of a new super-high strength steel. *J. Bull.Mater.Sci*. 26, 3, 301–305.
13. Karadeniz E, Ozsarac U and Yildiz C (2007) The effect of process parameters on penetration in gas metal arc welding processes. *J. Mater. & Des*. 28, 649–656.
14. Kim IS, Son JS, Kim IG, Kim JY and Kim OS (2003) A study on relationship between process variables and bead penetration for robotic CO_2 arc welding. *J. Mater. Process. Technol*. 136, 139–145.
15. Kim IS and *et al.* (2003) Sensitivity analysis for process parameters influencing weld quality in robotic GMA welding process. *J. Mater.Process.Technol.* 140, 676-681.
16. Lee JI and Um KW (2000) A prediction of welding process parameters by prediction of back-bead geometry. *J. Mater. Process. Technol*. 108, 106–113.
17. McGlone JC and Chadwick DB (1978) The submerged arc butt welding of mild steel. Part2.The prediction of weld bead geometry from the procedure parameters. *Welding Institute Report*. 80/1978/PE.
18. McGlone JC (1978) The submerged arc butt welding of mild steel. Part1. The influence of procedure parameters on weld bead geometry. *Welding Instt. Report*. 79/1978/PE.
19. Messler RW (1999) Principles of Welding, Processes, Physics, Chemistry, and Metallurgy. New York, John Wiley & Sons, Chapter 3.
20. Mostafa NB and Khajavi MN (2006) Optimization of welding parameters for weld penetration in FCAW. *J. Achieve.in Mater. and Man.Eng*. Vol.16, 1-2, 132-138.
21. Raveendra J and Parmar RS (1987) Mathematical models to predict weld bead geometry for flux cored arc welding. *J. Met. Construct*. 19, 31–35.
22. Roberts DK and Wells AA (1954) Fusion welding of aluminum alloys. *Brit.Weld J*. 1, 533–560.
23. Rosenthal D (1941) Mathematical theory of heat distribution during weld and cutting. Weld J. 20, 5, 220-s–234-s.
24. Shinoda T and Doherty J (1978) The relationships between arc welding parameters and weld bead geometry. *Welding Institute Report*. 74/1978/PE.
25. Tsao KC and Wu CS (1988) Fluid flow and heat transfer in GMA weld pools. *Weld J*. 67 , 3, 70s–75-s.
26. Yang LJ, Chandel RS and Bibby MJ (1993) The effects of process variables on the weld deposit area of submerged arc welds. *Weld J*. 72, 1, 11–18.
27. Zacharia T, Eraslan AH and Aidun DK (1988) Modeling of non-autogenous welding. *Weld J*. 67, 1, 18-s–27-s.